

# Analysis of stress singularity field near the cross point of inclusion and free surface by 3D element free Galerkin method (Influence of radius of curvature at vertex for stress singularity field)

**Takahiko Kurahashi<sup>1,\*</sup>, Yasuyuki Tsukada<sup>2</sup>, Hideo Koguchi<sup>2</sup>**

<sup>1</sup> Department of Mechanical Engineering, Nagaoka National College of Technology,  
888 Nishikatakai, Nagaoka, Niigata 940-8532, Japan

<sup>2</sup> Department of Mechanical Engineering, Nagaoka University of Technology,  
1603-1 Kamitomioka, Nagaoka, Niigata 940-2188, Japan

\* Corresponding author: kurahashi@nagaoka-ct.ac.jp

**Abstract** In this report, we investigate variation of stress distribution and intensity of stress singularity near the cross point of inclusion and free surface based on 3D element free Galerkin method (EFGM). We especially focus on influence of radius of curvature at vertex for stress singularity field. As for computational model, silicon and resin bonded structure is employed.

**Keywords** Stress distribution, Intensity of stress singularity, 3D EFGM, Radius of curvature at vertex

## 1. Introduction

Intensity of stress singularity near interface edge for bonded structures is investigated by a lot of researchers [1], [2]. Variation of intensity of stress singularity with respect to thickness of adhesive layer, interface width, slanted side surface have already investigated. As for the computational methods, the boundary element method (BEM) and the finite element method (FEM) are frequently used to compute stress distribution. In addition, the element free Galerkin method (EFGM) is also recently employed for stress analysis[3]. In this study, the EFGM is employed in stress analysis for bonded structures. In addition, eigen analysis based on the FEM is carried out to obtain order of stress singularity[4]. As the computational model, a structure made by resin with silicon plate inclusion is employed. We especially focus on influence of radius of curvature at vertex for stress singularity field in this study(See Fig.1).

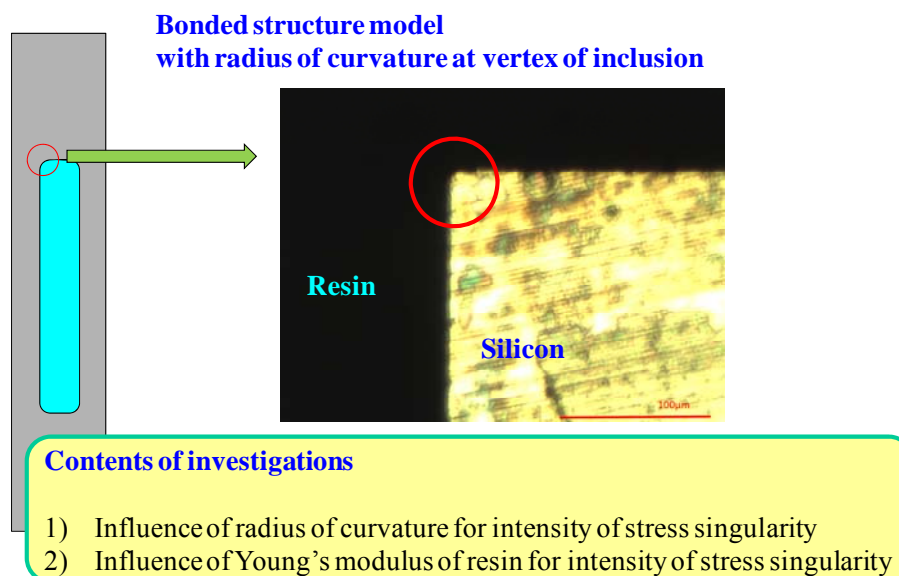


Figure 1. Image diagram of target model

## 2. Stress analysis by the EFGM and analysis of order of singularity by the FEM

The characteristics of the EFGM is that the interpolation function at evaluation point is given by the information in the domain influence (See Fig 2.). Example of the interpolation function is written as Eq. (1).

$$u(\mathbf{x}) = q_1(\mathbf{x})u_1 + q_2(\mathbf{x})u_2 + q_3(\mathbf{x})u_3 + \dots + q_n(\mathbf{x})u_n = \{q(\mathbf{x})\}^T \{u\}, \quad (1)$$

where  $q$  indicates shape function, and  $n$  indicates number of referred nodes in the domain influence. In addition, fourth order spline function is employed as the weighting function in the EFGM. Procedure of discretization is same as the traditional FEM. Detail of discretization is shown in reference [3].

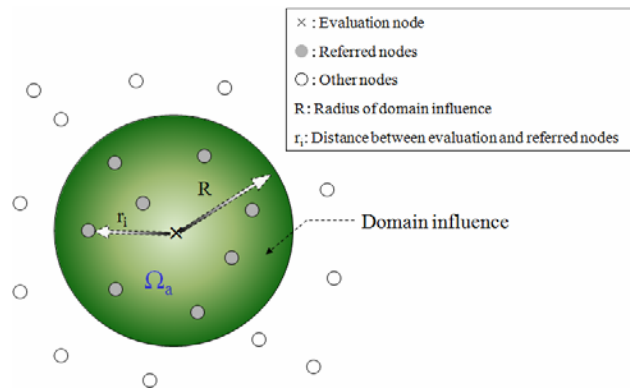


Figure 2. Domain influence

In addition, if the order of singularity is expressed by  $\lambda$ , the stress distribution is written as  $\sigma_{ij} \propto 1/r^\lambda = 1/r^{1-p} = r^{p-1}$ . Here,  $p$  indicates characteristic root. Because the stress is expressed as gradient of the displacements  $u_i$ , the relationship the displacements and distance  $r$  is given  $u_i \propto r^p$  by the integration of  $\sigma_{ij} \propto r^{p-1}$ . If displacements for each element are expressed by interpolation function shown in Eq. (2) and the interpolation function is substituted to equation of the principle of virtual work, a characteristic equation is finally derived as shown in Eq. (3).

$$\bar{u}_r(r, \theta, \phi) = \left( \frac{r}{r^0} \right)^p \sum_{i=1}^8 h_i \bar{u}_{ri}, \quad (2)$$

$$(p^2[\mathbf{A}] + p[\mathbf{B}] + [\mathbf{C}])\{\mathbf{x}\} = \{\mathbf{0}\}, \quad (3)$$

where  $\bar{u}_i$  is expressed by  $u_i - u_o$ , and  $u_i$  and  $u_o$  represent spherical displacements at an arbitrary point in the spherical surface. In addition,  $h_i$  indicates the shape function. In the Eq. (3),  $p$  indicates characteristic root and vector  $\{\mathbf{x}\}$  denotes superposed displacement vector in entire domain, and matrices  $[\mathbf{A}]$ ,  $[\mathbf{B}]$  and  $[\mathbf{C}]$  represent the coefficient matrices derived by finite element procedure. Detail of this formulation is shown in reference [4].

### 3. Numerical experiments

#### 3.1. Variation of intensity of stress singularity $K_{I\varphi\varphi}$ with respect to radius of curvature $R$

In this study, a structure made by resin with silicon plate inclusion shown in Fig.3 is employed as a numerical model. Nodal distribution around target area and material properties are shown in Fig.4 and Tab.1. In case of computational model of  $R=0$ , order of stress singularity  $\lambda$  at vertex on silicon surface is obtained as 0.436. In this study, the radius of curvature  $R$  at vertex of silicon plate is changed as shown in Tab.2.

In case that tensile stress, 10MPa, is applied to top surface, stress distribution  $\sigma_{\varphi\varphi}$  on surface in silicon plate with respect to angle  $\varphi$  is shown in Fig.5. It is seen that gradient of stress distribution  $\sigma_{\varphi\varphi}$  is almost same for each angle  $\varphi$ . Next, comparison of stress distribution  $\sigma_{\varphi\varphi}$  on silicon surface at angle direction  $\varphi=315^\circ$  is carried out. The result is shown in Fig.6. It is found that stress value decreases with increasing the radius of curvature  $R$  and constant stress region of  $\sigma_{\varphi\varphi}$  near point  $O$ , i.e., stress singularity disappearance region, increases with increasing the radius of curvature  $R$ . Here, in Fig. 6, solid line indicates fitting line by  $\sigma_{\varphi\varphi} = K_{I\varphi\varphi} r^{-0.436}$ . In addition, relationship between intensity of stress singularity  $K_{I\varphi\varphi}$  and radius of curvature  $R$  is shown in Fig.7. From this result, it is found that intensity of stress singularity  $K_{I\varphi\varphi}$  almost linearly decreases with increasing the radius of curvature  $R$ .

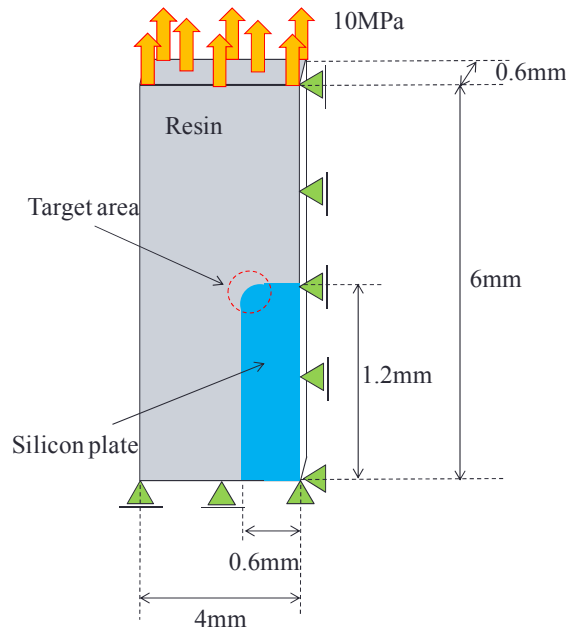


Figure 3. Computational model

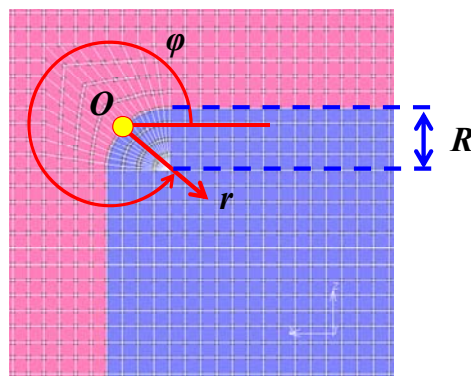


Figure 4. Nodal distribution around target area

Table 1. Material properties

	Silicon	Resin
Young's modulus (GPa)	166	5.49
Poisson's ratio	0.26	0.32

Table 2. Computational conditions

Radius of curvature R ( $\mu\text{m}$ )	0.000	3.125	6.250	12.500
Number of nodes	27,607	15,467	16,423	21,727

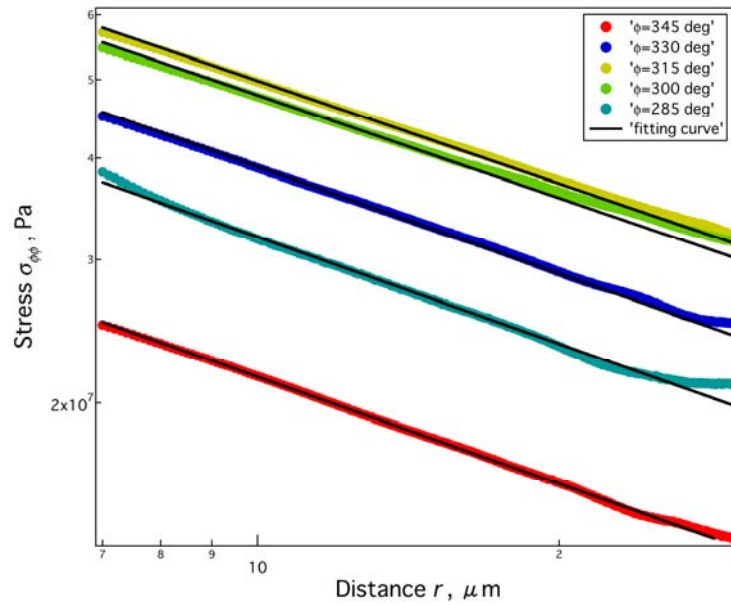


Figure 5. Variation of stress distribution  $\sigma_{\phi\phi}$  on silicon surface with respect to angle  $\phi$  ( $R=0\text{mm}$ )

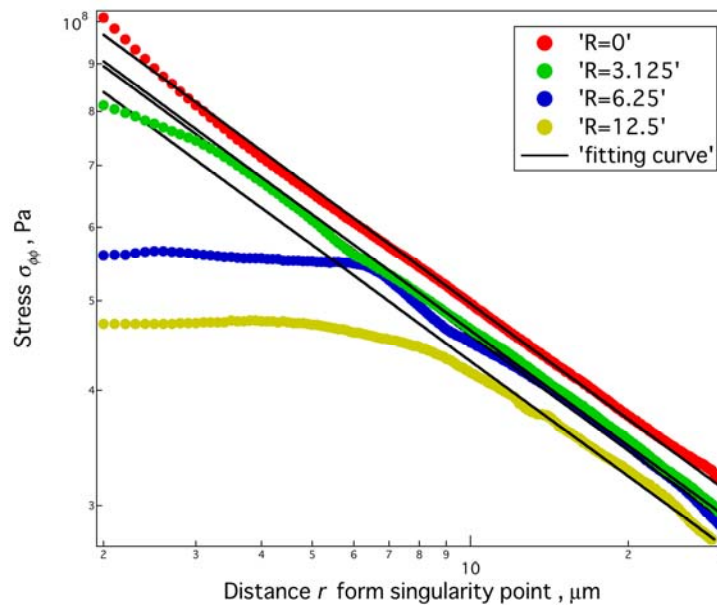


Figure 6. Variation of stress distribution  $\sigma_{\phi\phi}$  on silicon surface at angle direction  $\phi = 315^\circ$  with respect to radius of curvature  $R$

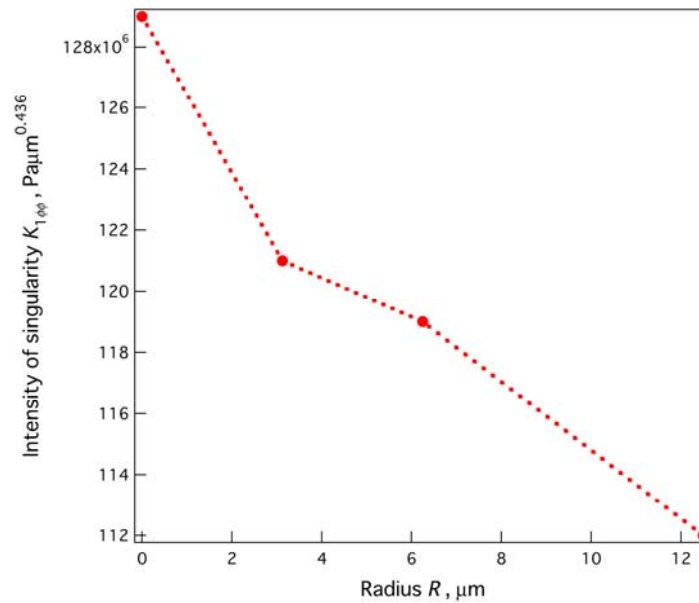


Figure 7. Relationship between intensity of stress singularity  $K_{1\varphi\varphi}$  and radius of curvature  $R$

### 3.2. Variation of intensity of stress singularity $K_{1\varphi\varphi}$ with respect to Young's modulus of resin

Next, in case of computational model,  $R=3.125\mu\text{m}$ , relationship between stress distribution and Young's modulus of resin is investigated. In this section, Young's modulus of silicon and resin are expressed by  $E_1$  and  $E_2$ . First of all, order of singularity  $\lambda$  is listed in Tab.3. It is seen that order of singularity  $\lambda$  gradually decreases with increasing Young's modulus of resin  $E_2$ . Fig.8 shows variation of stress distribution  $\sigma_{\varphi\varphi}$  on silicon surface at angle direction,  $\varphi = 315^\circ$ , with respect to Young's modulus of resin  $E_2$ . It is found that value of stress  $\sigma_{\varphi\varphi}$  decreases with increasing Young's modulus of resin  $E_2$ . In addition, variation of intensity of stress singularity  $K_{1\varphi\varphi}$  with respect to Young's modulus of resin  $E_2$  is shown in Fig.9. It is seen that intensity of stress singularity  $K_{1\varphi\varphi}$  decreases with increasing Young's modulus of resin  $E_2$ .

Table 3. Order of singularity  $\lambda$  (In case of  $R=0$  model)

Young's modulus of resin $E_2$ (GPa)	0.10	0.50	1.00	5.49	10.00
Order of singularity $\lambda$	0.545	0.437	0.429	0.436	0.384

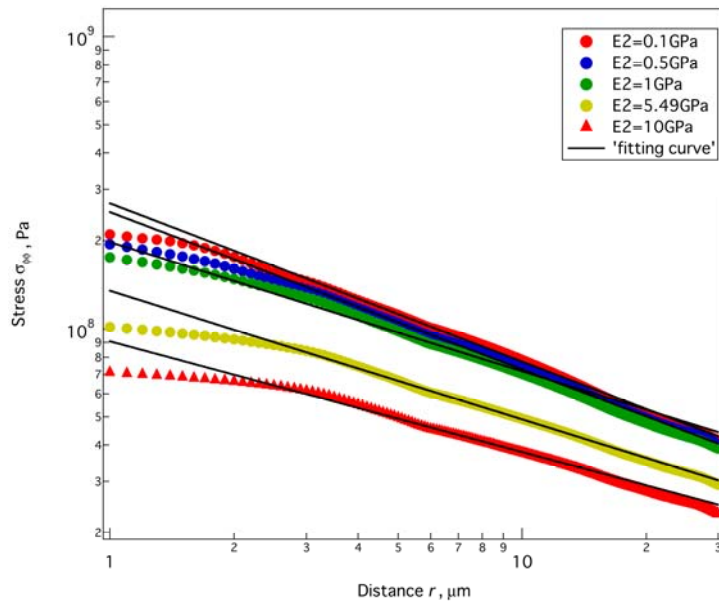


Figure 8. Variation of stress distribution  $\sigma_{\varphi\varphi}$  on silicon surface at angle direction  $\varphi = -45^\circ$  with respect to Young's modulus of resin

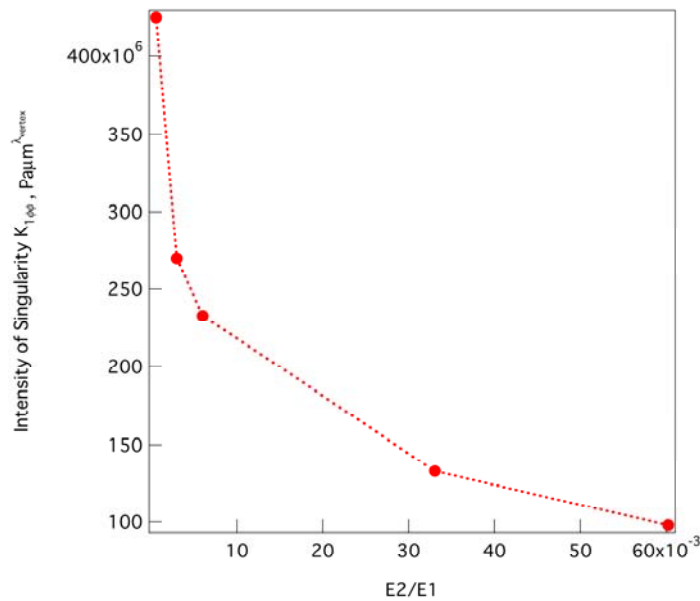


Figure 9. Variation of intensity of stress singularity  $K_{I\varphi\varphi}$  with respect to Young's modulus of resin  $E_2$

#### 4. Conclusins

In this study, we investigated about the relationship between intensity of singularity  $K_{I\theta\theta}$  and radius of curvature  $R$  for computational model of a structure made by resin with silicon plate inclusion. As numerical methods, the EFGM is applied to stress analysis, and the finite element eigen analysis is applied to obtain order of singularity at vertex on silicon surface. Conclusions in this study are shown below.

Examinations for change of radius of curvature around singularity point

- Stress value  $\sigma_{\varphi\varphi}$  decreases with increasing the radius of curvature  $R$ .
- Constant stress region of  $\sigma_{\varphi\varphi}$  near point  $O$ , i.e., stress singularity disappearance region, increases with increasing the radius of curvature  $R$ .
- Intensity of stress singularity  $K_{I\varphi\varphi}$  almost linearly decreases with increasing the radius of curvature  $R$ .

Examinations for change of Young's modulus of resin in case of  $R=3.125\mu\text{m}$  model

- Value of stress  $\sigma_{\varphi\varphi}$  decreases with increasing Young's modulus of resin  $E_2$ .
- Intensity of stress singularity  $K_{I\varphi\varphi}$  decreases with increasing Young's modulus of resin  $E_2$ .

### References

- [1] T. Kurahashi, A. Ishikawa and H. Koguchi, Evaluation of Intensity of Stress Singularity for 3D Dissimilar Material Joints Based on Mesh Free Method, 11th International Conference on the Mechanical Behavior of Materials, *Procedia Engineering*, 10, (2011) 3095-3100 .
- [2] Hideo Koguchi, Kazuhisa Hoshi, Evaluation of joining strength of silicon-resin interface at a vertex in 3D joint structures, *InterPACK2011*, (2011).
- [3] T.Belytschko, Y.Y.Lu and L.Gu, Element-free Galerkin methods, *Int. J. Numer. Meth. Engrg.*, 37(5), (1994) 229-256.
- [4] S.S.Pageau and S.B.Bigger,JR, Finite element evaluation of free - edge singular stress fields in anisotropic materials, *Int.J.Numer.in Engng.*, 38, (1995) 2225-2239.